PROBING THE CKM TRIANGLE AT BaBar*

G. Eigen

for the BaBar Collaboration

University of Bergen
Allégaten 55, 5007 Bergen, Norway

(Received November 21, 2003)

We present recent BaBar measurements that constrain both the sides and the angles of the Unitarity Triangle.

PACS numbers: 11.30.Er, 12.15.Ah

1. Introduction

In the Standard Model (SM) CP violation results from Yukawa couplings of the Higgs field to the quark fields that are introduced to produce fermion masses. The quark mass matrix is diagonalized by four unitary transformations. In the charged-weak current the interactions with the W boson to the quarks becomes flavor diagonal in the basis of weak eigenstates. The latter are related to mass eigenstates by the unitary Cabbibo–Kobayashi–Maskawa (CKM) matrix V_{ij} [1,2], where the first (second) index denotes an up-type (down-type) quark. A convenient representation of CKM matrix is the Wolfenstein parameterization [3], which to order $O(\lambda^5)$ is given by:

$$V = \begin{pmatrix} 1-\frac{\lambda^2}{2}-\frac{\lambda^4}{8} & \lambda & A\lambda^3(\rho - i\eta) \\ -\lambda + A^2\lambda^5(\frac{1}{2}-\rho-i\eta) & 1-\frac{\lambda^2}{2}-\frac{\lambda^4}{8}(1+4A^2) & A\lambda^2 \\ A\lambda^3(1-\bar{\rho}-i\bar{\eta}) & -A\lambda^2 + A\lambda^4(\frac{1}{2}-\rho-i\eta) & 1-\frac{1}{2}A^2\lambda^4 \end{pmatrix} + O(\lambda^6). \tag{1}$$

Of the four parameters $\lambda = 0.2235 \pm 0.0033$, is the best measured, $A \simeq 0.82$ is known to $\sim \pm 5\%$, while $\bar{\rho} = \rho(1-\lambda^2/2)$ and $\bar{\eta} = \eta(1-\lambda^2/2)$ are poorly known. In the SM, $\bar{\eta}$ represents the CP-violating phase. Unitarity of CKM matrix yields six triangular relations, of which $V_{ud}V_{ub}^* + V_{cd}V_{cb}^* + V_{td}V_{tb}^* = 0$ is the most useful, since it specifies a triangle in the $\bar{\rho} - \bar{\eta}$ plane with apex $\bar{\rho}, \bar{\eta}$ and sides of similar length.

---

* Presented at the XXVII International Conference of Theoretical Physics, "Matter to the Deepest", Ustroń, Poland, September 15–21, 2003.

The BaBar experiment has been running since May 1999 and by now has recorded an integrated luminosity of $\mathcal{L}_{\rm tot} = 131.3$ fb^{-1} on the $\Upsilon(4S)$ peak and $\mathcal{L}_{\rm tot} = 12.5$ fb^{-1} in the continuum 40 MeV below the $\Upsilon(4S)$ peak. This luminosity corresponds to a $B\bar{B}$ sample of $\sim 1.42 \times 10^8$ events. The performance of the BaBar detector is described elsewhere [4].

Since in the $\Upsilon(4S)$ rest frame B mesons are produced nearly at rest, we can take advantage of two kinematic variables, $m_{\rm ES} = \sqrt{E^{*2}_{\rm beam} - p^{*2}_B}$ and $\Delta E = E^*_B - E^*_{\rm beam}$, where $E^*_{\rm beam}$ and E^*_B (p^*_B) respectively denote the beam energy and the energy (momentum) of the reconstructed B meson in the $\Upsilon(4S)$ rest frame. In the $\Delta E - m_{\rm ES}$ plane signal events will cluster around $\Delta E = 0$ and $m_{\rm ES} = m_B$, while backgrounds from other B decays and $q\bar{q}$ continuum typically show no peaking behavior in the signal region.

2. Measurement of $|V_{cb}|$

The CKM matrix element $|V_{cb}|$ is extracted from semileptonic decays involving charm quarks. The inclusive decay rate to order $O(1/m_B^2)$ is predicted by the heavy quark expansion (HQE) [5]:

$$\begin{aligned}\Gamma(B \to X_c \ell\nu) \;=\; & \frac{G_{\rm F}^2|V_{ub}|^2}{192\pi^3} 0.369 m_B^5 \times \Bigg[1 - 1.54\frac{\alpha_{\rm s}}{\pi} - 1.65\frac{\bar{\Lambda}}{m_B}\left(1 - 0.87\frac{\alpha_{\rm s}}{\pi}\right) \\ & -0.95\frac{\bar{\Lambda}^2}{m_B^2} - 3.18\frac{\lambda_1}{m_B^2} + 0.02\frac{\lambda_1}{m_B^2} + O\left(\frac{\Lambda_{\rm QCD}}{m_B}\right)^3\Bigg], \qquad (2)\end{aligned}$$

where $G_{\rm F}$ is the Fermi constant and $\bar{\Lambda}$, λ_1 and λ_2 are non-perturbative HQE parameters. Intuitively, $\bar{\Lambda}$ denotes the energy of the light-quark and gluon degrees of freedom, λ_1/m_B represents the average kinetic energy of the b-quark inside the B meson, and λ_2/m_B denotes the hyperfine interaction of the b-quark spin with the spin of the light degrees of freedom. The B meson mass can be expanded in terms of the b quark mass and the HQE parameters, $m_B = m_b + \bar{\Lambda} - (\lambda_1 + 3\lambda_2)/(2m_b)$. Similarly, hadronic-mass moments and lepton-energy moments can be expressed in terms of HQE parameters. Measuring the hadronic-mass moment m_X^2, we can determine $\bar{\Lambda}$ and λ_1 if we specify λ_2 and the next-order HQE parameters.

Following a method pioneered by CLEO [6], BaBar has measured the m_X and m_X^2 moment distributions in semileptonic $B \to X_c\ell\nu$ decays using $8.9 \times 10^7 B\bar{B}$ pairs [7]. In the recoil of fully reconstructed B mesons in different hadronic final states, we select events that have exactly one lepton with momentum $p^* > 0.9$ GeV in the B rest frame. The missing four-momentum in the event serves as an estimator for the ν four-momentum ($p_{\rm miss} = p_\nu$) in a two-constraints kinematic fit, where we require equal masses for the reconstructed and recoil B mesons and zero missing-mass squared ($m^2_{\rm miss} = 0$). For $m_{\rm ES} > 5.27$ GeV 7,114 candidates are retained above a background of 2,102 events. The resulting m^2_X distribution (for $p^* > 0.9$ GeV) corrected for combinatorial backgrounds is shown in figure 1(a).

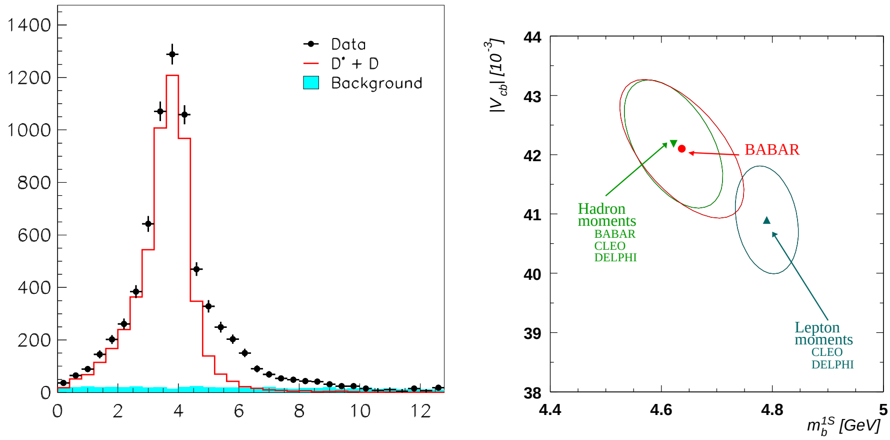

Fig. 1. (a) The measured M^2_X distribution for $p^*_{\rm min} = 0.9$ GeV after subtracting combinatorial backgrounds. The histogram shows the dominant D and D^* contributions and the shaded area indicates residual background. (b) Constraints on HQE parameters from the measured semileptonic decay rate and the m^2_X distribution projected into the $V_{cb} - m_b$ plane. For comparison, combined measurements for hadronic-mass moments from BaBar , CLEO and DELPHI and lepton-energy moments from CLEO and DELPHI are also shown.

To extract $\bar{\Lambda}$ and λ_1, we perform a χ^2 minimization of the m^2_X moment distributions for seven different lepton threshold momenta, where we fixed $\lambda_2 = 0.128 \pm 0.01$ GeV^2, $T_i = 0$ GeV^3, $\rho_1 = 1/2(0.5)^3$ GeV^3 and expressed ρ_2 in terms of T_2, T_4, and the D^*–D and B^*–B mass splittings [8]. Using the $\overline{\rm MS}$ scheme [5] we extract $\bar{\Lambda}^{\overline{\rm MS}} = (0.53 \pm 0.09_{\rm exp})$ GeV and $\lambda_1^{\overline{\rm MS}} = (0.36 \pm 0.09_{\rm exp})$ GeV^2. A combined fit to the hadronic-mass moments and the semileptonic width $\Gamma_{\rm sl} = (4.37 \pm 0.18) \times 10^{-11}$ MeV in the $\Upsilon(1S)$ mass scheme [9] yields $m_b(1S) = (4.638 \pm 0.094_{\rm exp} \pm 0.090_{\rm th})$ GeV, $\lambda_1 = (0.26 \pm 0.06_{\rm exp} \pm 0.06_{\rm th})$ GeV^2, and $|V_{cb}| = (42.10 \pm 1.04_{\rm exp} \pm 0.72_{\rm th}) \times 10^{-3}$. While the first error results from all experimental uncertainties, the second error denotes uncertainties from perturbative effects [10], dimensional analysis and $1/m_b^3$ corrections summed in quadrature. The $V_{cb} - m_b$ contour is plotted in figure 1(b) showing good agreement with results of other experiments [6,11,12]. The world average for inclusive measurements yields $|V_{cb}| = (42.0 \pm 0.5_{\rm exp} \pm 0.9_{\rm th}) \times 10^{-3}$ [13].

In exclusive $B \to D^*\ell\nu$ decays, $|V_{cb}|$ is extracted from the phase-space corrected decay rate at zero recoil. Heavy quark effective theory (HQET) [14] predicts the value at zero recoil to be $|V_{cb}|\mathcal{F}_{D^*}(1)$ [15], where $\mathcal{F}_{D^*}(1) = 0.91 \pm 0.04$ is the universal form factor for finite b-quark mass at zero recoil [16,17]. BaBar measures $|V_{cb}|\mathcal{F}_{D^*}(1) = (34.1 \pm 1.3) \times 10^{-3}$ yielding $|V_{cb}| = (37.5 \pm 1.4_{\rm exp} \pm 1.6_{\rm th}) \times 10^{-3}$ [18], which is consistent with the world average for exclusive measurements of $|V_{cb}| = (40.2 \pm 0.8_{\rm exp} \pm 1.8_{\rm th}) \times 10^{-3}$ [13]. Within errors, exclusive and inclusive $|V_{cb}|$ measurements are consistent.

3. Measurement of $|V_{ub}|$

The CKM matrix element $|V_{ub}|$ is measured in charmless semileptonic B decays. In HQE [19], V_{ub} is related to the branching fraction by

$$|V_{ub}| = 0.00445 \left(\frac{\mathcal{B}(B \to X_u\ell\nu)}{0.002} \, \frac{1.55 \text{ ps}}{\tau_b} \right)^{1/2} \times (1.0 \pm 0.02_{\rm pert} \pm 0.052_{1/m_b^3}). \tag{3}$$

Since the branching fraction $\mathcal{B}(B \to X_u\ell\nu)$ is only 2% of $\mathcal{B}(B \to X_c\ell\nu)$ [20], we need to look at kinematic regions that are depleted in the $B \to X_c\ell\nu$ background. Besides the lepton endpoint spectrum [21] and $B \to \rho\ell\nu$ [22], BaBar has explored the hadronic-mass m_X below the D meson [21]. Using the fully reconstructed hadronic B meson sample selected from 8.9×10^7 $B\bar{B}$ decays, we look for events that contain an identified lepton ($p^* > 1.0$ GeV) in the recoil and perform ν reconstruction. To minimize the $B \to X_c\ell\nu$ background, events with a $K^\pm$ or a $K^0_{\rm S}$ are rejected. We measure the ratio of branching fractions $R_u = \mathcal{B}(B \to X_u\ell\nu)/\mathcal{B}(B \to X\ell\nu)$ to reduce experimental systematic effects. The total sample of semileptonic candidates comprises 29,982 events. Figure 2(a) shows the observed hadronic-mass spectrum. A χ^2 fit with the $B \to X_u\ell\nu$ signal shape, a $B \to X_c\ell\nu$ background shape and other background contributions (hadrons misidentified as leptons, secondary τ decays or charm decays) yields 175 ± 21 signal candidates for $m_X < 1.55$ GeV. The background-subtracted spectrum is displayed in figure 2(b).

For $m_X < 1.55$ GeV we measure $R_u = (2.06 \pm 0.25_{\rm stat} \pm 0.26_{\rm sys} \pm 0.36_{\rm th})\%$, where the theory error is obtained by varying the non-perturbative parameters $\bar{\Lambda}$ and λ_1 within their uncertainties including a -0.8 correlation between them [6,24]. We further measure a charmless inclusive branching fraction of $\mathcal{B}(B \to X_u\ell\nu) = (2.24 \pm 0.27_{\rm stat} \pm 0.26_{\rm sys} \pm 0.39_{\rm th}) \times 10^{-3}$, that yields $|V_{ub}| = (4.62 \pm 0.28_{\rm stat} \pm 0.27_{\rm sys} \pm 0.49_{\rm th}) \times 10^{-3}$. Our result agrees with other inclusive V_{ub} measurements, as shown in figure 3 [13]. My weighted average of inclusive measurements is $|V_{ub}| = (4.20 \pm 0.12_{\rm exp} \pm 0.60_{\rm th}) \times 10^{-3}$, where

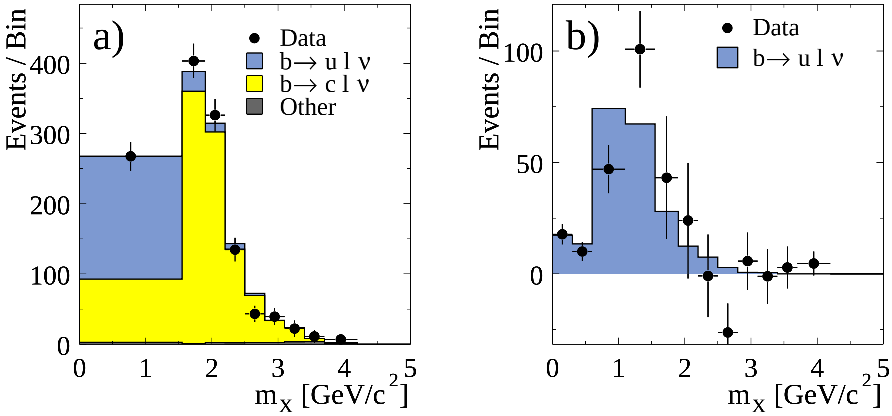

Fig. 2. The m_X distribution for $\bar{B} \to X\ell^-\bar{\nu}$ candidates; (a) data (points) and fit components and (b) data after subtraction of $b \to c\ell\nu$ and the other backgrounds.

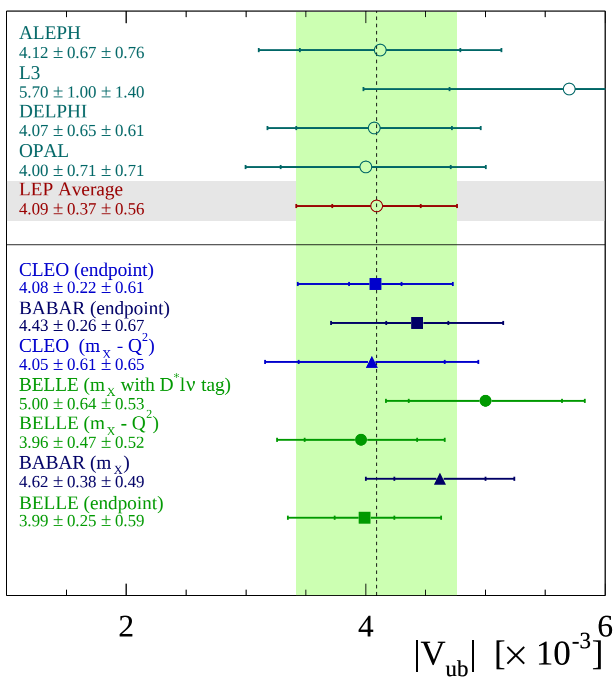

Fig. 3. Comparison of inclusive $|V_{ub}|$ measurements (compiled by HFAG).

the theoretical uncertainty is obtained by taking the difference of weighted means with the theoretical uncertainty added linearly and the weighted V_{ub} average, $\Delta^{\rm th}_{V_{ub}} = \langle V_{ub} + \Delta_{V_{ub}}\rangle - \langle V_{ub}\rangle$.

4. Measurement of $|V_{td}|$

The CKM matrix element V_{td} is obtained from the $B^0_d\bar{B}^0_d$ oscillation frequency Δm_{B_d}, which has been measured in several experiments with different methods [13]. BaBar has measured Δm_{B_d} using dileptons [25], a $B \to D^*\ell\nu$ sample [26] and a fully reconstructed B-meson sample [27]. For the same luminosity, the dilepton sample yields the most precise result for the oscillation frequency Δm_{B_d}, which is extracted from the time-dependent asymmetry of opposite-sign and same-sign dileptons originating from unmixed and mixed $B\bar{B}$ events, respectively:

$$A(\Delta t) = \frac{N_{\ell^+\ell^-}(\Delta t) - N_{\ell^\pm\ell^\mp}(\Delta t)}{N_{\ell^+\ell^-}(\Delta t) + N_{\ell^\pm\ell^\mp}(\Delta t)} \propto \cos(\Delta m_{B_d}\Delta t)\,. \tag{4}$$

The time difference between the two B decays, Δt, is computed from the nominal boost and the spatial separation of the two B decay vertices, $\Delta z = z_2 - z_1$. The decay vertices are determined from the positions of closest approach to the primary vertex in the transverse plane, which is obtained for each event from a vertex fit of the two lepton tracks and the beam spot constraint. To parameterize the measured asymmetry, we have to convolve $N_{\ell\ell}$ with the time resolution function and include all backgrounds. The largest background comes from B^+B^- decays (50%), which have no oscillatory term and mainly contribute to $N_{\ell^+\ell^-}$. Another large source is $b \to c \to \ell$ cascade decays, while contributions from J/ψ decays, $q\bar{q}$ continuum and hadrons misidentified as leptons are found to be small.

In a sample of 2.3×10^7 $B\bar{B}$ events, BaBar [25] has selected 99,010 dilepton events after significantly reducing background of leptons from cascade decays with the help of a neural network. The sample has a purity of 87% and a efficiency of 9%. The time-dependent asymmetry is plotted in figure 4. The oscillation frequency is extracted from a binned maximum likelihood fit to the data sample with the requirement $|\Delta t| < 12$ ps, yielding $\Delta m_{B_d} = (0.493 \pm 0.012_{\rm stat} \pm 0.009_{\rm sys})\ \hbar{\rm ps}^{-1}$. The dominant systematic errors result from the B lifetimes and the time-dependence of the resolution function.

Using 14,000 reconstructed $B^0 \to D^{*-}\ell^+\nu$ events, BaBar [26] measured $\Delta m_{B_d} = (0.492 \pm 0.018_{\rm stat} \pm 0.013_{\rm sys})\ \hbar{\rm ps}^{-1}$. Both results are in good agreement with the world average of $\Delta m_{B_d} = (0.502 \pm 0.006)\ \hbar{\rm ps}^{-1}$ [13].

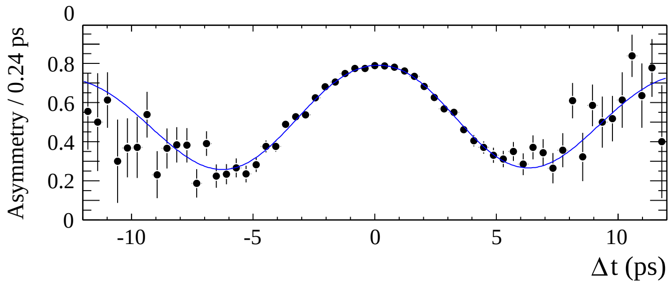

Fig. 4. Time-dependent asymmetry between opposite-sign and same-sign dileptons.

5. Measurement of $\sin 2\beta$

The theoretical cleanest CP violation measurements in the $B\bar{B}$ system produced at the $\Upsilon(4S)$ are obtained for CP eigenstates f that have a single amplitude. Here, CP violation is caused by the interference of the direct decay $B^0 \to f$ with the decay after mixing $B^0 \to \bar{B}^0 \to f$. The relevant parameter is [28]

$$\lambda_f = \eta_f \, \frac{q}{p} \, \frac{\bar{A}_{\bar{f}}}{A_f} \,, \tag{5}$$

where η_f is the CP eigenvalue of f, $q/p \approx \mathrm{e}^{-2i\beta}$ is the mixing phase and $\bar{A}_{\bar{f}}/A_f$ is the amplitude ratio. CP violation occurs, if $\lambda_f \neq \pm 1$ or if $\mathcal{I}m\lambda \neq 0$, which are both sufficient and necessary conditions for $\Gamma(\bar{B}^0(\Delta t) \to f_{\mathrm{CP}})$ and $\Gamma(B^0(\Delta t) \to f)$ to differ. We basically distiguish among three types of CP violation: *(i)* CP violation in decay which is also called direct CP violation ($\bar{A}_{\bar{f}}/A_f \neq \pm 1$), *(ii)* CP violation in mixing ($q/p \neq \pm 1$), and *(iii)* CP violation in the interference between decays with and without mixing ($\mathcal{I}m\lambda \neq 0$).

Generally, the time-dependent CP asymmetry is expressed by [28]:

$$\begin{aligned} a_{\mathrm{CP}}(\Delta t) &= \frac{\Gamma(\bar{B}^0(\Delta t) \to f) - \Gamma(B^0(\Delta t) \to f)}{\Gamma(\bar{B}^0(\Delta t) \to f) + \Gamma(B^0(\Delta t) \to f)} \\ &= -C_f \, \cos(\Delta m_{B_d} \Delta t) + S_f \, \sin(\Delta m_{B_d} \Delta t) \,, \end{aligned} \tag{6}$$

where $C_f = (1 - |\lambda_f|^2)/(1 + |\lambda_f|^2)$ and $S_f = 2\mathcal{I}m\lambda_f/(1 + |\lambda_f|^2)$. In case of a single amplitude with $|\lambda_f| = 1$, the first term vanishes and the time dependence is solely governed by the sine term. It is important to measure the time dependence of the CP asymmetry, since the time-integrated CP asymmetry vanishes. The experimental separation between $\Gamma(\bar{B}^0(\Delta t) \to f)$ and $\Gamma(B^0(\Delta t) \to f)$ depends upon how well the b flavor can be tagged at production and upon the shape of the time resolution function. For example, the mistag rate w and the resolution function $\mathcal{R}(\Delta t)$ can be measured independently in $B\bar{B}$ mixing analyses [25,26]. Experimentally, a time-dependent

CP-violation measurement basically involves three steps: *(i)* kinematic reconstruction of one B in a CP eigenstate, *(ii)* flavor tagging of the other B at production and *(iii)* measurement of the time difference Δt between the two decay vertices [29]. Since the B mesons are boosted in BaBar ($\beta\gamma = 0.55$), we need to determine the decay vertex separation along the boost direction (z).

The golden mode for measuring $\sin 2\beta$ is $B^0 \to J/\psi K^0_{\rm S}$. Since the tree amplitude dominates, we encounter a single weak phase (β) expecting negligible direct CP violation ($|\lambda_{\psi K_{\rm S}}| = 1 + \mathcal{O}(10^{-3})$ [28] and the CP asymmetry is simply given by $\sin 2\beta \sin(\Delta m_{B_d} t)$. Experimentally, $B \to J/\psi K^0_{\rm S}$ has a large branching fraction and can be cleanly reconstructed with high efficiency. Other charmonium $K^0_{\rm S}$ ($K^0_{\rm L}$) eigenstates are rather suitable as well.

In a sample of 8.8×10^7 $B\bar{B}$ pairs, BaBar [30] has measured the CP asymmetry in charmonium $K^0_{\rm S}$ ($K^0_{\rm L}$) modes. We reconstruct the CP-odd eigenstates $B^0 \to J/\psi K^0_{\rm S}$, $B^0 \to \psi(2S) K^0_{\rm S}$, $B^0 \to \chi_{c1} K^0_{\rm S}$, and $B^0 \to \eta_c K^0_{\rm S}$ with $K^0_{\rm S} \to \pi^+\pi^-$, $K^0_{\rm S} \to \pi^0\pi^0$ (only for J/ψ final states), $\psi(2S) \to e^+e^-, \mu^+\mu^-$ or $J/\psi\pi^+\pi^-$, $\chi_{c1} \to \gamma J/\psi$, $J/\psi \to e^+e^-$ or $\mu^+\mu^-$, and $\eta_c \to K\bar{K}\pi$. We reconstruct the CP-even eigenstate $J/\psi K^0_{\rm L}$ [31]. After vertex requirements and flavor tagging we retract 1,506 CP-odd signal candidates with a purity of 94% and 988 CP-even signal candidates with a purity of 55%. In addition, we detect 147 events in $B^0 \to J/\psi K^{*0}$ with $K^{*0} \to K^0_{\rm S}\pi^0$ [32]. The $J/\psi K^{*0}$ decay is a vector vector mode that has mixed symmetry requiring a transversity angle analysis [33] to separate the CP-even and CP-odd eigenstates. The CP-odd component was measured to be $R_\perp = 0.16 \pm 0.035$, yielding $\eta_f = 0.65 \pm 0.07$ after corrections.

B flavor tagging at production utilizes charge correlation of a primary lepton or a kaon and the b quark flavor. For example, a primary $e^+(\mu^+)$ produced in $B^0 \to D^{*-}\ell^+\nu$ and similarly a K^+ that is produced in the cascade $B^0 \to \bar{D}X, \bar{D} \to K^+Y$ originates from a $\bar{b}$ quark. In addition, the charge of the slow π^- is anticorrelated with the $\bar{b}$ quark flavor.

For each event we combine the information on number of leptons, kaons and slow pions along with tracking, particle identification, and kinematics information into a neural network. We classify each event into four mutually exclusive tagging categories: lepton, kaon I, kaon II and inclusive category [29]. The relevant parameter is the effective tagging efficiency, $Q = \epsilon(1-2w)$, which combines the reconstruction efficiency with the mistag rate, because the error on $\sin 2\beta$ is affected by Q as $\sigma(\sin 2\beta) \sim 1/\sqrt{Q}$. We measure $Q = (7.9 \pm 0.3)\%$ (lepton), $Q = (10.7 \pm 0.4)\%$ (kaon I), $Q = (6.7 \pm 0.4)\%$ (kaon II) and $Q = (2.7 \pm 0.3)\%$ (inclusive), yielding total tagging efficiency of $Q = (28.1 \pm 0.7)\%$ [29]. While the lepton category has the highest purity, the kaon categories have the highest efficiency.

For a boost of $\beta\gamma = 0.55$, the average vertex separation is $\langle \Delta z \rangle = 254\ \mu$m [29], while the typical resolution for measuring Δz is $\sigma = 180\ \mu$m. The time distributions and CP asymmetry of charmonium $K^0_{\rm S}$ and $J/\psi K^0_{\rm L}$ CP eigenstates are displayed in figure 5. Performing a 34-parameter unbinned maximum likelihood fit to the time distribution of the full CP sample (2,461 events) and a sample of fully reconstructed B hadronic final states (25,375 events), BaBar measures $\sin(2\beta) = 0.741 \pm 0.067_{\rm stat} \pm 0.033_{\rm syst}$ [30]. Our result is in perfect agreement with a recent Belle measurement [34].

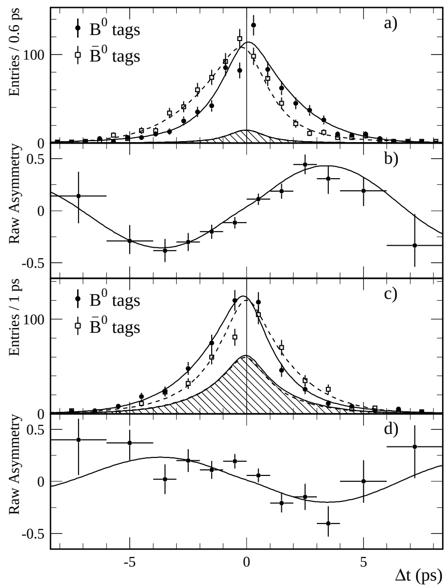

Fig. 5. Comparison of the measured $\bar{B}^0$ and B^0 decay time distributions for (a) $\eta_f = -1$ and (c) $\eta_f = +1$ CP eigenstates of charmonium K^0 modes and the corresponding time-dependent CP asymmetries (b,d). The solid lines represent projections of the maximum likelihood fits and the shaded regions represent backgrounds.

In the SM $b \to c\bar{c}d$ processes, such as $B \to J/\psi\pi^0$ or $B \to D^{(*)\pm}D^{(*)\mp}$, the weak phase is the same as that for $B \to J/\psi K^0_{\rm S}$. The measurements, however, may differ from $\sin 2\beta$ because of additional phases from non-negligible penguin amplitudes. The CP asymmetry is parameterized with both the sine and cosine terms, where $S_f = \sin 2\beta_{\rm eff}$. We have measured CP asymmetries in $B \to J/\psi\pi^0$ [35], $B \to D^{*\pm}D^{\mp}$ [36], and $B \to D^{*\pm}D^{*\mp}$ [37]. The latter mode requires a transversity angle analysis to separate CP-even and CP-odd eigenstates. The results are summarized in Table I. Presently, the errors are too large to draw definite conclusions on direct CP violation. In $B \to D^{*+}D^{*-}$, $S_{D^*D^*}$ is 2.5σ below the SM expectation.

In the SM, CP eigenstates that originate from $b \to s\bar{s}s$ processes also measure $\sin 2\beta$. Theoretically, $B \to \phi K^0_{\rm S}$ is the cleanest mode, since both the leading and sub-dominant mode are penguin loops with the t quark dominating as shown in figure 6 (u quark contribution is 0.02) [38]. Rescattering contributions are expected to be small [39]. In the SM, one expects at most a 5% deviation for $S_{\phi K^0_{\rm S}}$ from $\sin 2\beta$ measured in $B \to J/\psi K^0_{\rm S}$. $B \to \phi K^0_{\rm S}$ is rather sensitive to new physics, as additional diagrams with new heavy particles in the penguin loop may produce deviations from the SM prediction [40]. Experimentally, we need a high luminosity to be sensitive to deviations, since the branching fraction is very small. BaBar has selected 70 ± 9 $\phi K^0_{\rm S}$ signal events in a sample of 1.24×10^8 $B\bar{B}$ pairs. For a selection efficiency of 7.4%, this yields a branching fraction of $\mathcal{B}(B \to \phi K^0_{\rm S} = (7.6^{+1.3}_{-1.2} \pm 0.5) \times 10^{-6}$ [41].

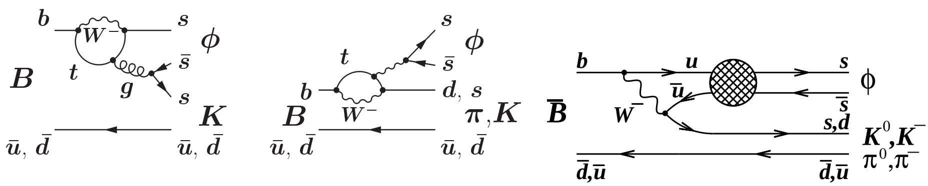

Fig. 6. SM penguin diagrams and rescattering diagram for $B \to \phi K^0_{\rm S}$.

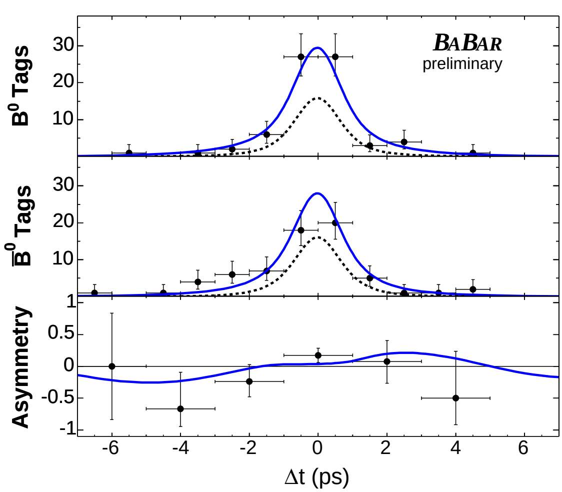

Fig. 7. Measured time dependence of $\bar{B}^0$ and B^0 decays and the CP asymmetry for $B \to \phi K^0_{\rm S}$. The dotted curves represent the background contribution.

Figure 7 shows the time dependence of the $\bar{B}^0$ and B^0 decay rates and the resulting CP asymmetry. A maximum likelihood fit yields $S_{\phi K^0_S} = 0.45 \pm 0.43_{\rm stat} \pm 0.07_{\rm sys}$, and $C_{\phi K^0_S} = -0.38 \pm 0.37_{\rm stat} \pm 0.12_{\rm sys}$, which is consistent with the SM prediction. Using 1.5×10^8 $B\bar{B}$ pairs, Belle [42] measured $S_{\phi K^0_S} = -0.96 \pm 0.50_{\rm stat}\ {}^{+0.09}_{-0.11\ \rm sys}$, which deviates by 3.5σ from the $\sin 2\beta$ world average for charmonium K^0_S (K^0_L) eigenstates. Averaging both experiments yields $S_{\phi K^0_S} = -0.14 \pm 0.33$, which is 2.6σ below the present $\sin 2\beta$ world average for charmonium K^0_S (K^0_L) eigenstates and thus is still consistent with the SM.

The CP eigenstate $B \to \eta' K^0_S$ has an order of magnitude larger branching fraction than $\mathcal{B}(B \to \phi K^0_S)$. In a sample of 8.8×10^7 $B\bar{B}$ events, BaBar measured $\mathcal{B}(B \to \eta' K^0_S = (55.4 \pm 5.2 \pm 4.0) \times 10^{-6}$ [43]. Here, however, the sub-dominant processes include a $b \to u$ tree diagram, which is estimated to be of the order of $|T/P| \approx (8 \pm 3)\%$ [44]. Table I summarizes all BaBar measurements of S_f and C_f or $|\lambda_f|$. Figure 8 shows the world average of $\sin 2\beta_{\rm eff}$ measurements compiled by the heavy flavor averaging group (HFAG). At the present level of precision all S_f measurements are consistent with the SM.

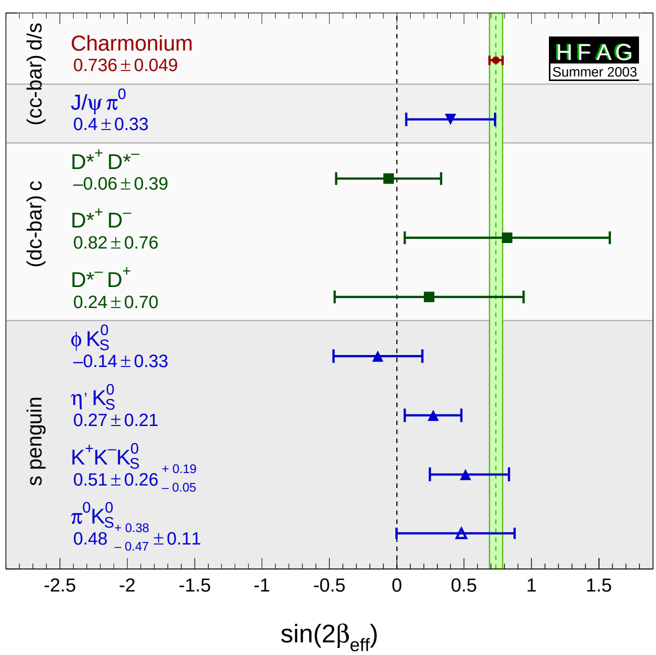

Fig. 8. Compilation of $\sin 2\beta_{\rm eff}$ measurements by HFAG for different CP eigenstates averaged over BaBar and Belle.

TABLE I

Summary of BaBar measurements for parameters of the CP asymmetry S_f and C_f or $|\lambda_f|$ (Eq. (6)) obtained in different CP eigenstates originating from $b \to c\bar{c}s$, $b \to s\bar{s}s$, and $b \to c\bar{c}d$ processes. In addition, the order of magnitude of branching fractions is shown as well as the dominant decay amplitude in bold face.

Mode	$\mathcal{B}[10^{-6}]$	$\mathcal{A}$	Yields	S_f	C_f or $(\lvert\lambda_f\rvert)$
$J/\psi K^0_S$	440	$\boldsymbol{T}$	2461	$0.741 \pm 0.067 \pm 0.033$	$(0.95 \pm 0.05 \pm 0.03)$
$\eta' K^0_S$	29	$\boldsymbol{P} + T$	203 ± 19	$0.02 \pm 0.34 \pm 0.03$	$0.10 \pm 0.22 \pm 0.04$
ϕK^0_S	4	$\boldsymbol{P}$	70 ± 9	$0.45 \pm 0.43 \pm 0.07$	$-0.38 \pm 0.37 \pm 0.12$
$J/\psi \pi^0$	20	$\boldsymbol{T} + P$	40 ± 7	$0.05 \pm 0.49 \pm 0.16$	$0.38 \pm 0.41 \pm 0.08$
$D^{*+}D^-$	900	$\boldsymbol{T} + P$	113 ± 13	$-0.82 \pm 0.75 \pm 0.14$	$-0.47 \pm 0.40 \pm 0.12$
D^+D^{*-}	900	$\boldsymbol{T} + P$		$-0.24 \pm 0.69 \pm 0.12$	$-0.22 \pm 0.37 \pm 0.10$
$D^{*+}D^{*-}$	1000	$\boldsymbol{T} + P$	156 ± 14	$0.05 \pm 0.29 \pm 0.10$	$(0.75 \pm 0.19 \pm 0.02)$

6. Measurement of $\sin 2\alpha$

In order to determine the angle α, we need to measure time-dependent CP asymmetries of $b \to u\bar{u}d$ processes, such as $B \to \pi^+\pi^-$, $B \to \rho\pi$, $B \to \rho\rho$ [28]. Penguin pollution, however, generally complicates the extraction of α [45]. In $B \to \pi^+\pi^-$, we expect $P/T \sim 30\%$. Leading-order and subdominant Feynman diagrams for $B \to \pi\pi$ are depicted in figure 9. The CP asymmetry $a_{\pi\pi}$ contains both the cosine and sine terms and $S_{\pi\pi}$ measures $\sin 2\alpha_{\rm eff}$, where $2\alpha_{\rm eff} = 2\alpha + \Delta\phi$. Using the Gronau–London method [45], $\Delta\phi$ can be determined by a $B \to \pi\pi$ isospin analysis [46] that requires to measure six branching fractions: $B^0 \to \pi^+\pi^-$, $B^0 \to \pi^0\pi^0$, $B^+ \to \pi^+\pi^0$, $\bar{B}^0 \to \pi^+\pi^-$, $\bar{B}^0 \to \pi^0\pi^0$ and $B^- \to \pi^-\pi^0$. Via isospin relations, the amplitudes of B and $\bar{B}$ decays form two triangles as shown in figure 10. Since the amplitudes of the charged B decays are solely determined by the tree diagram, their absolute values are equal providing a common basis for the two triangles. The angle between the two triangles defines $\Delta\phi$. Inclusion of electroweak penguin processes slightly modifies the extraction of α [47].

The decays $B^0 \to \pi^+\pi^-$ and $B^+ \to \pi^+\pi^0$ have been measured by CLEO [58], BaBar [49, 50] and Belle [51]. For example, BaBar measures branching fractions of $\mathcal{B}(B^0 \to \pi^+\pi^-) = (4.7 \pm 0.6 \pm 0.2) \times 10^{-6}$ [49] and $\mathcal{B}(B^+ \to \pi^+\pi^0) = (5.5^{+1.0}_{-0.9} \pm 0.5) \times 10^{-6}$ [50] for the $\pi^+\pi^-$ and $\pi^+\pi^0$ modes, respectively. Recently, evidence for $B \to \pi^0\pi^0$ was also found by BaBar [52] and Belle [53]. Analyzing 1.24×10^8 $B\bar{B}$ pairs, BaBar selected $46 \pm 13 \pm 3$ $\pi^0\pi^0$ candidates (a 4.2σ significance) yielding a rather large branching fraction of $\mathcal{B}(B^0 \to \pi^0\pi^0) = (2.1 \pm 0.6 \pm 0.3) \times 10^{-6}$.

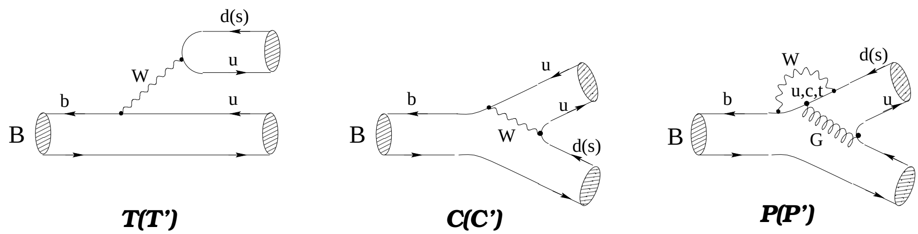

Fig. 9. Leading-order and subdominant Feynman diagrams for $B \to \pi\pi$ decays.

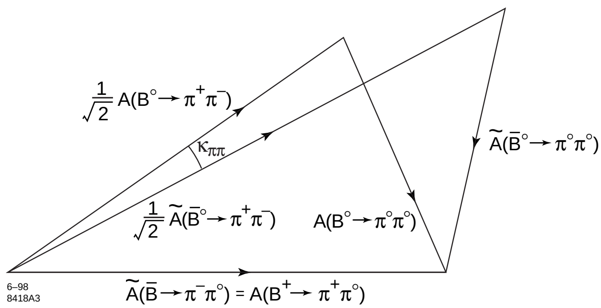

Fig. 10. Isospin relation for $B \to \pi\pi$ and $\bar{B} \to \pi\pi$ decays.

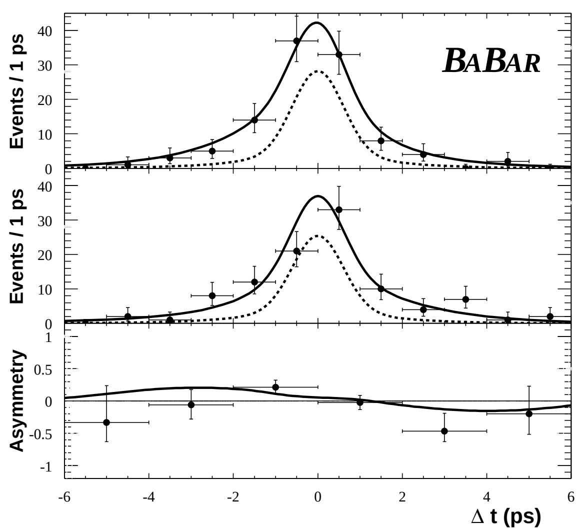

Fig. 11. BaBar measurement of the Δt distribution for $\bar{B}^0$ and B^0 decays to the $\pi^+\pi^-$ final state and the CP asymmetry. The solid curve shows the projection of the fit and the dotted curves represent the background contribution.

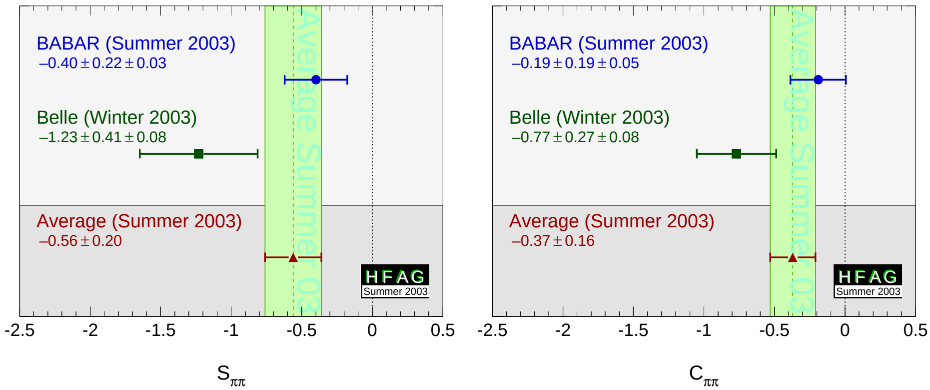

Fig. 12. Comparison of $S_{\pi\pi}$ and $C_{\pi\pi}$ measurements from BaBar and Belle.

For a sample of 1.24×10^8 $B\bar{B}$ pairs, BaBar measured the time-dependent $\bar{B}^0$ and B^0 decay rates and the CP asymmetry for $B \to \pi^+\pi^-$ as shown in figure 12. A maximum likelihood fit to the CP asymmetry yields $C_{\pi\pi} = -0.19 \pm 0.19 \pm 0.05$ and $S_{\pi\pi} = -0.40 \pm 0.22 \pm 0.03$ [54]. Without an isospin analysis we can presently place an upper bound on $\Delta\phi$ of $|\alpha_{\rm eff} - \alpha| < 48^\circ$. In order to extract α from $\alpha_{\rm eff}$ with a precision of $\sigma(\Delta\phi) = 5^\circ$, a sample of the order of 10^{10} $B\bar{B}$ events is required [55]. Our results differ from the Belle measurements [56] as shown in figure 12. The present world average is consistent with the expected value for α obtained from sides of the unitarity triangle and $\sin 2\beta$. In the near future a Dalitz plot analysis in $B \to \rho\pi$ may provide additional information on α.

7. Measurement of γ

The ratios of branching fractions involving $B \to K\pi$ or $B \to \pi\pi$ decays bear sensitivity to the angle γ. As an example, figure 13 shows the predictions of QCD factorization [57] for $R_k = \mathcal{B}(B^0 \to K^\pm\pi^\mp)/(2\,\mathcal{B}(B^0 \to K^0\pi^0))$, $R_c = \mathcal{B}(B^0 \to \pi^\pm\pi^\mp)/(2\,\mathcal{B}(B^\pm \to \pi^\pm\pi^0)) \times \tau_{B^\pm}/\tau_{B^0}$, and $R_n = \mathcal{B}(B^0 \to \pi^0\pi^0)/\mathcal{B}(B^\pm \to \pi^\pm\pi^0) \times \tau_{B^\pm}/\tau_{B^0}$. Using average values for the $K\pi$ and $\pi\pi$ branching fractions listed in Table II, we determine $R_k = 0.79 \pm 0.1$, $R_c = 0.48 \pm 0.08$ and $R_n = 0.47 \pm 0.12$. While the measurement of R_k prefers small values of γ ($< 50^\circ$), the measurement of R_c prefers γ values above 70°. The measurement of R_n excludes all values of γ at the 1.67σ level (see figure 13).

Another method for measuring γ is based upon $D^0\bar{D}^0$ mixing between a color-allowed Cabbibo-suppressed $b \to c\bar{u}s$ transition and a color-suppressed Cabbibo-allowed $b \to u\bar{c}s$ transition that both are order $O(\lambda^3)$ processes. This idea, for example, is utilized in $B^\pm \to DK^\pm$ transitions depicted in

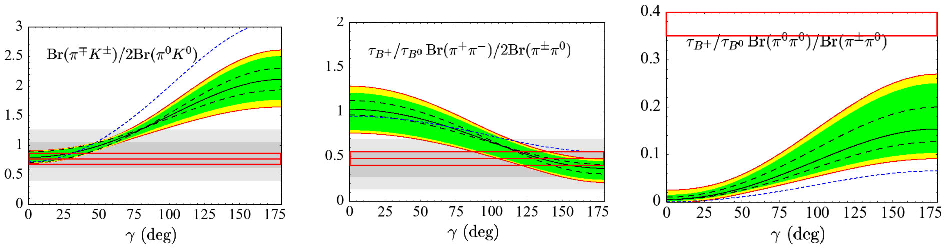

Fig. 13. Predictions from QCD factorization [57] for R_k, R_c and R_n in comparison to recent measurements shown as black lines (central value plus error bars). Note that in the right-hand plot the central value lies outside the figure.

TABLE II

Branching fraction measurements of charmless $B \to K\pi$ and $B \to \pi\pi$ decays from BaBar [49], Belle [51], and CLEO [58].

Mode	BaBar $\mathcal{B}[10^{-6}]$	Belle $\mathcal{B}[10^{-6}]$	CLEO $\mathcal{B}[10^{-6}]$	Average $\mathcal{B}[10^{-6}]$
$K^\pm\pi^\mp$	$17.9 \pm 0.9 \pm 0.7$	$18.5 \pm 1.0 \pm 0.7$	$18.0^{+2.3+1.2}_{-2.1-0.9}$	17.9 ± 1.0
$K^0\pi^0$	$10.4 \pm 1.5 \pm 0.8$	$12.6 \pm 2.4 \pm 1.4$	$12.8^{+4.0+1.7}_{-3.3-1.4}$	11.3 ± 1.3
$K^\pm\pi^0$	$12.8^{+1.2}_{-1.0} \pm 1.0$	$12.8 \pm 1.4^{+1.4}_{-1.0}$	$12.9^{+2.4+1.2}_{-2.2-1.1}$	12.8 ± 1.1
$K^0\pi^\mp$	$17.5^{+1.8}_{-1.7} \pm 1.3$	$22.0 \pm 1.9 \pm 1.1$	$18.8^{+3.7+2.1}_{-3.3-1.8}$	19.7 ± 1.5
$\pi^\pm\pi^\mp$	$4.7 \pm 0.6 \pm 0.2$	$4.4 \pm 0.6 \pm 0.3$	$4.5^{+1.4+0.5}_{-1.2-0.4}$	4.6 ± 0.4
$\pi^0\pi^0$	$2.1 \pm 0.6 \pm 0.3$	$1.7 \pm 0.6 \pm 0.3$	< 4.4	2.0 ± 0.5
$\pi^\pm\pi^0$	$5.5^{+1.0}_{-0.9} \pm 0.5$	$5.3 \pm 1.3 \pm 0.5$	$4.6^{+1.8+0.7}_{-1.6-0.6}$	5.2 ± 0.8

figure 14 [59]. The amplitudes of the decays $B^- \to D^0K^-$, $B^- \to \bar{D}^0K^-$ and $B^- \to D^0_{\rm CP}K^-$ form a triangle, where $D^0_{\rm CP}$ denotes a CP eigenstate. For example, we can reconstruct CP-even eigenstates (D^0_+) in decays such as $D^0_+ \to \pi^+\pi^-$ or $D^0_+ \to K^+K^-$. Another triangle is obtained for the corresponding B^+ decays. Since the color-allowed $b \to c$ transition involves no weak phase, the amplitudes $\mathcal{A}(B^- \to D^0K^-)$ and $\mathcal{A}(B^+ \to D^0K^+)$ are identical. Using the amplitude $\mathcal{A}(B^- \to D^0K^-)$ as a common basis for both triangles, the opening angle between them is 2γ, as shown in figure 15.

To determine γ, we measure the following ratio of branching fractions

$$R_{\rm CP} = \frac{\mathcal{B}(B^- \to D^0_{\rm CP}K^-) + \mathcal{B}(B^+ \to D^0_{\rm CP}K^+)}{\mathcal{B}(B^- \to D^0K^-) + \mathcal{B}(B^+ \to D^0K^+)} = 1 + r^2_{\rm DK} \pm 2r_{\rm DK}\cos\delta\cos\gamma \tag{7}$$

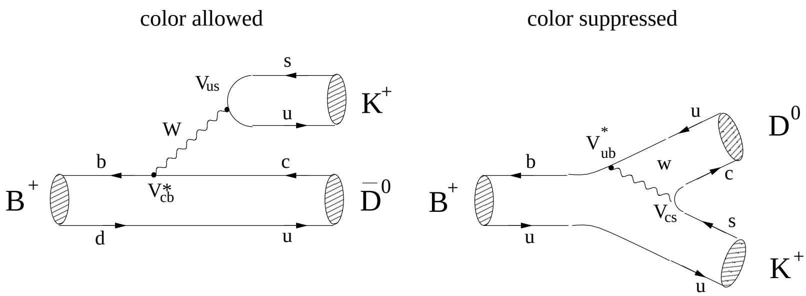

Fig. 14. Leading-order Feynman diagrams for $B^+ \to \bar{D}^0 K^+$ and $B^+ \to DK^+$.

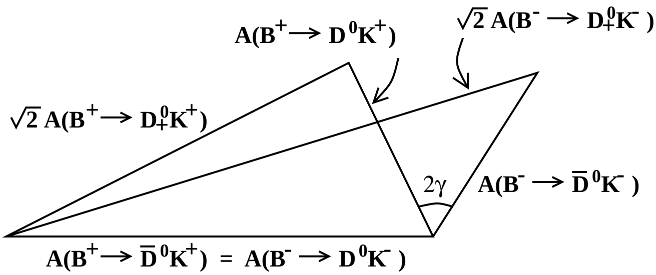

Fig. 15. Triangular relations for $B^\pm \to DK^\pm$ amplitudes.

and the CP asymmetry

$$A_{\rm CP} = \frac{\mathcal{B}(B^- \to D^0_{\rm CP}K^-) - \mathcal{B}(B^+ \to D^0_{\rm CP}K^+)}{\mathcal{B}(B^- \to D^0_{\rm CP}K^-) + \mathcal{B}(B^+ \to D^0_{\rm CP}K^+)} = \frac{2r_{\rm DK}\sin\delta\sin\gamma}{R_{\rm CP}}\,, \tag{8}$$

where we denote the strong phase by δ and the ratio of color-suppressed amplitudes by $r_{\rm DK} = |\mathcal{A}(B^- \to \bar{D}^0 K^-)|/|\mathcal{A}(B^+ \to D^0 K^+)|$. In addition to γ, both δ and $r_{\rm DK}$ ($\simeq 0.1-0.3$) are also unknown. BaBar has measured these quantities for the CP-even D^0 state, yielding $R_+ = 0.89 \pm 0.21 \pm 0.08$ and $A_+ = 0.17 \pm 0.23^{+0.09}_{-0.07}$ [54]. The ratio of Cabbibo-suppressed to Cabbibo--allowed decays amount to

$$\frac{\mathcal{B}(B^\pm \to D^0_{\rm CP}K^\pm)}{\mathcal{B}(B^\pm \to D^0_{\rm CP}\pi^\pm)} = (7.4 \pm 1.7 \pm 0.6)\%$$

and

$$\frac{[\mathcal{B}(B^+ \to \bar{D}^0K^+) + \mathcal{B}(B^- \to D^0K^-)]}{[\mathcal{B}(B^+ \to \bar{D}^0\pi^+) + \mathcal{B}(B^- \to D^0\pi^-)]} = (8.31 \pm 0.35 \pm 0.2)\%\,.$$

In order to determine the three unknown parameters γ, δ and $r_{\rm DK}$, $R_{\rm CP}$ and $A_{\rm CP}$ also need to be measured for CP-odd D^0 eigenstates, such as $K^0_{\rm S}\pi^0$

or $K_S^0\phi$ states. Assuming $r_{\rm DK} = 0.3$, the errors are presently too large to constrain γ. For a luminosity of $\mathcal{L} = 0.5$ (2.0) ab^{-1}, we expect a precision of $\sigma(\sin^2\gamma) = 0.32$ (0.2) for $r_{\rm DK} = 0.3$ [63].

The angle γ can be also extracted by measuring the time-dependent decays rates of $\bar{B}^0 \to D^{(*)+}\pi^-$ [61]. Here, the color-allowed process ($O(\lambda^2)$) interferes with the color-suppressed process ($O(\lambda^4)$) after $B\bar{B}$ mixing. The B^0 and $\bar{B}^0$ time-dependent decays rates are given by:

$$\Gamma(B^0 \to D^{\mp}\pi^{\pm}, \Delta t) = N\mathrm{e}^{-|\Delta t|/\tau_{B^0}}\Big[1 \pm C\cos(\Delta m_{B_d^0}\Delta t) + S^{\mp}\sin(\Delta m_{B_d^0}\Delta t)\Big]$$

$$\Gamma(\bar{B}^0 \to D^{\mp}\pi^{\pm}, \Delta t) = N\mathrm{e}^{-|\Delta t|/\tau_{B^0}}\Big[1 \mp C\cos(\Delta m_{B_d^0}\Delta t) - S^{\mp}\sin(\Delta m_{B_d^0}\Delta t)\Big], \tag{9}$$

where $C = (1 - r_{D\pi}^2)/(1 + r_{D\pi}^2)$, $S^{\mp} = (2r_{D\pi})/(1 + r_{D\pi}^2)\sin(2\beta + \gamma \pm \delta)$ and $r_{D\pi} = \mathcal{A}(\bar{B}^0 \to D^-\pi^+)/\mathcal{A}(B^0 \to D^-\pi^+) \approx 0.02$. Using 8.8×10^7 $B^0\bar{B}^0$ decays BaBar has studied both $B^0 \to D^{\mp}\pi^{\pm}$ and $B^0 \to D^{*\mp}\pi^{\pm}$ decays. Using a maximum likelihood fit to the Δt distributions of $\bar{B}^0$ and B^0 decays to $D^{(*)\mp}\pi^{\pm}$ final states, BaBar measures the following combinations [60]

$$\begin{aligned}
2r_{D^*\pi}\sin(2\beta+\gamma)\cos\delta_{D^*\pi} &= -0.068 \pm 0.038 \pm 0.021,\\
2r_{D^*\pi}\sin(2\beta+\gamma)\sin\delta_{D^*\pi} &= -0.031 \pm 0.070 \pm 0.035,\\
2r_{D\pi}\sin(2\beta+\gamma)\cos\delta_{D\pi} &= -0.022 \pm 0.038 \pm 0.021,\\
2r_{D\pi}\sin(2\beta+\gamma)\sin\delta_{D\pi} &= -0.025 \pm 0.068 \pm 0.035.
\end{aligned} \tag{10}$$

From these results we determine $\sin(2\beta+\gamma) > 0.69$@ 68.3% confidence level (C.L.).

8. Present status of the unitarity triangle

Figure 16 shows the present status of the unitarity triangle, where we have included world average measurements of $\mathcal{B}(B \to X_c\ell\nu)$, $\mathcal{B}(B \to D^*\ell\nu)$, $\mathcal{B}(B \to X_u\ell\nu)$, $\mathcal{B}(B^0 \to \rho^{\mp}\ell^{\pm}\nu)$, Δm_{B_d}, ϵ_K and $\sin 2\beta = 0.736 \pm 0.049$ measured in charmonium $K_{\rm S}^0$ ($K_{\rm L}^0$) CP eigenstates [20] [64]. We further include the information of $B_s^0\bar{B}_s^0$ mixing, where we use a new parameterization based on the significance of observing Δm_{B_s} in the present LEP and SLD amplitude measurements [13]. The method is discussed in detail in reference [64]. A χ^2 minimization is used to determine the parameters $\bar{\rho}$, $\bar{\eta}$, A of the CKM matrix. The prediction of observables in terms of Wolfenstein parameters involves theoretical parameters, such as reduced rates for the branching fractions, $f_B\sqrt{B_B}$, B_K and ξ [28], which are affected by non-Gaussian uncertainties. We include terms that take care of correlations among the observables

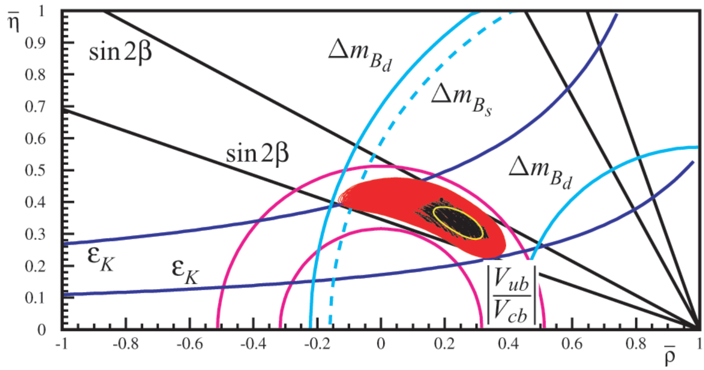

Fig. 16. Present status of the unitarity triangle. The black points represent a $\bar{\rho}, \bar{\eta}$ central value obtained from an individual χ^2 fit, the dark-shaded region shows an overlay of the corresponding 95% C.L. contours, while the light ellipse indicates a typical shape of a 95% C.L. contour. Also shown are the 95% bounds on $|V_{ub}/V_{cb}|$, Δm_{B_d}, Δm_{B_s}, ϵ_K and $\sin 2\beta$.

and the Gaussian errors in the theoretical parameters. The explicit values of the observables and theoretical parameters are listed in reference [64]. We perform a particular χ^2 fit with fixing the theoretical parameters to specific values within their allowed region, which we call a "model". We perform χ^2 fits for many different models scanning over the entire non-Gaussian range for each of the theoretical parameters. We accept only models that have a fit probability of $P(\chi^2) > 5\%$). The light-colored ellipse in Figure 16 represents a 95 % C.L. contour of a typical fit. The black region shows the most-probable (central) value for $\bar{\rho}, \bar{\eta}$ for each model accepted, while the dark-shaded region represents the overlay of the 95% C.L. contours of all accepted models. In order to guide the eye we also show individual 95% C.L. bounds for $|V_{ub}/V_{cb}|$, Δm_{B_d}, Δm_{B_s}, ϵ_K, and $\sin 2\beta$.

This procedure allows us to place non-Gaussian ranges and experimental errors on the Wolfenstein parameters and angles of the unitarity triangle, yielding $0.103_{-0.067} \leq \bar{\rho} \leq 0.337^{+0.026}$, $0.280_{-0.020} \leq \bar{\eta} \leq 0.409^{+0.034}$, $0.80_{-0.024} \leq A \leq 0.85^{+0.027}$, $(83.1_{-16.6})^\circ \leq \alpha \leq (130.0^{+5.4})^\circ$, and $(40.4_{-3.2})^\circ \leq \gamma \leq (74.5^{+8.3})^\circ$. In our notation, the non-Gaussian uncertainties are denoted by a range and the experimental uncertainties are shown on top as one-sided errors. Additional measurements of $\sin 2\alpha$ and γ in the future will further overconstrain the unitarity triangle. Adding information of CP asymmetries of $B \to \phi K^0_{\rm S}$ will provides a crucial test of the SM, once the precision on $S_{\phi K^0_{\rm S}}$ is improved. The ultimate test of the SM, however, will be to check if $\alpha + \beta + \gamma = \pi$. To achieve a precision of the order of 5°, we will need a luminosity of 30–50 ab^{-1}.

9. Conclusion

About three years after the start of the B factories, $\sin 2\beta$ measured in charmonium $K^0_{\rm S}$ ($K^0_{\rm L}$) eigenstates is becoming a precision measurement. $\sin 2\beta_{\rm eff}$ measured in $B \to D^{*+}D^{*-}$ decays may indicate the presence of penguin processes. The present results of $\sin 2\beta$ measured in $B \to \phi K^0_{\rm S}$ look interesting, but the errors are too large to draw conclusions concerning new physics phases. The determination of $\sin 2\alpha$ is complicated due to the presence of penguin amplitudes. In order to separate $\sin 2\alpha$ from $\sin 2\alpha_{\rm eff}$ measured in the CP asymmetry $a_{\pi^+\pi^-}$, an integrated luminosity of tens of ab^{-1} is needed. The determination of γ in $B^\pm \to D^0_{\rm CP}K^\pm$ final states or from time-dependent CP asymmetries of $B^0 \to D^{(*)-}\pi^+$ modes is even more difficult. The $B \to K\pi$ and $B \to \pi\pi$ branching fractions may already indicate a problem with QCD factorization in the BBNS model [57] and require further investigation with increased luminosities.

Inclusive analysis methods for $B \to X_u \ell\nu$ and $B \to X_c \ell\nu$ allow the extraction of $|V_{ub}|$ and $|V_{cb}|$ with a reduced model dependence. The extraction of $|V_{td}|$ will depend on improvements of the non-Gaussian uncertainties in $f_{B_d}\sqrt{B_{B_d}}$. In the future, the ratio of branching fractions $\mathcal{B}(B \to \rho\gamma)/\mathcal{B}(B \to K^*\gamma)$ may provide additional constraints on $|V_{td}|/|V_{ts}|$ [65]. Presently, the precision of the $\bar\rho - \bar\eta$ plane is determined by theoretical uncertainties. In order to reduce the allowed region in the $\bar\rho - \bar\eta$ plane, we need both precision measurements and reduced non-Gaussian theoretical uncertainties. In the future, measurements of $\sin 2\alpha$ and γ will provide further constraints on the unitarity triangle. The ultimate test, however, will consist of checking the relation $\alpha + \beta + \gamma = \pi$. With increasing luminosity the uncertainties of CP asymmetries will decrease. While for charmonium $K^0_{\rm S}$ ($K^0_{\rm L}$) CP eigenstates the uncertainty at $\mathcal{L} = 50$ ab^{-1} is expected to level off around $\sigma(\sin 2\beta) \sim 1.5\%$ due to dominating systematic errors, we expect to reach a precision for $B \to \phi K^0_{\rm S}$ of $\sigma(\sin 2\beta) < 3\%$ (for $\sin 2\beta = 0.736$) [66]. The precision for $a_{\pi\pi}$ is expected to be $\sigma(\alpha) \sim$ few$\,^\circ$, while that of the CP violating asymmetry in $B \to D^{(*)}\pi$ will be of the order of 3% [55].

I would like to thank the organizers of the conference for their hospitality and conference arrangements. The BaBar collaboration I would like to thank for support in arranging this talk. In particular I would like to thank Bob Cahn, David Hitlin, Gautier Hamel de Monchenault and Antimo Palano for fruitful discussions. This work has been supported by the Norwegian Research Council.

REFERENCES

[1] N. Cabbibo, *Phys. Rev. Lett.* **10**, 531 (1963).

[2] M. Kobayashi, T. Maskawa, *Prog. Theor. Phys.* **49**, 652 (1973).

[3] L. Wolfenstein, *Phys. Rev. Lett.* **51**, 1945 (1983).

[4] BaBar Collaboration, (B. Aubert *et al.*), *Nucl. Instrum. Methods* **A479**, 1 (2002).

[5] A. F. Falk, M.E. Luke, *Phys. Rev.* **D57**, 424 (1998).

[6] CLEO Collaboration, (D. Cronin-Hennessy *et al.*), *Phys. Rev. Lett.* **87**, 251808 (2001).

[7] BaBar Collaboration, (B. Aubert *et al.*), SLAC-PUB-10067, `hep-ex/0307046`.

[8] M. Gremm, A. Kapustin, *Phys. Rev.* **D55**, 6924 (1997).

[9] C.W. Bauer, Z. Ligeti, M. Luke, A.V. Manohar, *Phys. Rev.* **D67**, 054012 (2003).

[10] S.J. Brodsky, G.P. Lepage, P.B. Mackenzie, *Phys. Rev.* **D28**, 228 (1983).

[11] CLEO Collaboration, (R.A. Briere *et al.*), `hep-ex/0209024`.

[12] DELPHI Collaboration, (M. Calvi *et al.*), `hep-ex/0210046`.

[13] http://www.slac.stanford.edu/xorg/hfag/.

[14] N. Isgur, M. Wise, *Phys. Lett.* **237**, 527 (1990); A.F. Falk, H. Georgi, B. Grinstein, M.B. Wise, *Nucl. Phys.* **B343**, 1 (1990); M. Neubert, *Phys. Lett.* **B264**, 455 (1991); M. Neubert, *Phys. Lett.* **B338**, 84 (1994).

[15] A.F. Falk, M. Neubert, *Phys. Rev.* **D47**, 2965 and 2982 (1993); T. Mannel, *Phys. Rev.* **D50**, 428 (1994); M.A. Shifman, N.G. Uraltsev, M.B. Voloshin, *Phys. Rev.* **D51**, 2217 (1995).

[16] A. Czarnecki, *Phys. Rev. Lett.* **76**, 4126 (1996).

[17] S. Hashimoto *et al.*, *Phys. Rev.* **D66**, 014503 (2002).

[18] BaBar Collaboration (B. Aubert *et al.*), SLAC-PUB-10105, 22pp, `hep-ex/0308027`.

[19] V.D. Barger, C.S. Kim, R.J. Phillips, *Phys. Lett.* **B251**, 629 (1990); A.F. Falk, Z. Ligeti, M. B. Wise, *Phys. Lett.* **B406**, 225 (1997); R.D. Dikeman, N.G. Uraltsev, *Nucl. Phys.* **B509**, 378 (1998); I.I. Bigi, R.D. Dikeman, N. Uraltsev, *Eur. Phys. J.* **C4**, 453 (1998).

[20] Particle Data Group, K. Hagiwara *et al.*, *Phys. Rev.* **D66**, 010001 (2002).

[21] BaBar Collaboration (B. Aubert *et al.*), SLAC-PUB-9282, 17pp, `hep-ex/0207081`.

[22] BaBar Collaboration (B. Aubert *et al.*), *Phys. Rev. Lett.* **90**, 181801 (2003).

[23] BaBar Collaboration (B. Aubert *et al.*), SLAC-PUB-10045, 7pp, `hep-ex/0307062`.

[24] F. De Fazio, M. Neubert, *J. High Energy Phys.* **9906**, 017 (1999).

[25] BaBar Collaboration (B. Aubert *et al.*), *Phys. Rev. Lett.* **88**, 231801 (2003).

[26] BaBar Collaboration (B. Aubert *et al.*), *Phys. Rev.* **D67**, 072002 (2003).

[27] BaBar Collaboration (B. Aubert *et al.*), *Phys. Rev. Lett.* **88**, 221802 (2002).

[28] BaBar Collaboration (P.F. Harrison, H.R. Quinn, eds.) SLAC-R-0504 (1998).

[29] BaBar Collaboration (B. Aubert *et al.*), *Phys. Rev.* **D66**, 032003 (2002).

[30] BaBar Collaboration (B. Aubert *et al.*), *Phys. Rev. Lett.* **89**, 201802 (2002).

[31] BaBar Collaboration, (B. Aubert *et al.*), SLAC-PUB-9170, `hep-ex/0203040`.

[32] BaBar Collaboration, (B. Aubert *et al.*), *Phys. Rev. Lett.* **87**, 241801 (2001).

[33] I. Dunietz *et al.*, *Phys. Rev.* **D43**, 2193 (1991); A.S. Dighe *et al.*, *Phys. Lett.* **B369**, 144 (1996).

[34] Belle Collaboration (K. Abe *et al.*), Belle-conf-0353 9 pp, `hep-ex/0308037`.

[35] BaBar Collaboration (B. Aubert *et al.*), *Phys. Rev. Lett.* **91**, 061802 (2003).

[36] BaBar Collaboration (B. Aubert *et al.*), *Phys. Rev. Lett.* **90**, 221801 (2003).

[37] BaBar Collaboration (B. Aubert *et al.*), *Phys. Rev. Lett.* **91**, 131801 (2003).

[38] N.G. Deshpande, J. Trampetic, *Phys. Rev.* **D41**, 895 (1990); N.G. Deshpande, X.-G. He, *Phys. Lett.* **B336**, 471 (1994); R. Fleischer, *Z. Phys.* **C62**, 81 (1994).

[39] Y. Grossman, G. Isidori, M.P. Worah, *Phys. Rev.* **D58**, 057504 (1998).

[40] Y. Grossman, M.P. Worah, *Phys. Lett.* **B395**, 241 (1997); R. Fleischer, *Int. J. Mod. Phys.* **A12**, 2459 (1997).

[41] BaBar Collaboration (B. Aubert *et al.*), SLAC-PUB-9684, `hep-ex/0303029`.

[42] Belle Collaboration (K. Abe *et al.*), KEK-PREPRINT-2003-47, 10 pp, `hep-ex/0308035`.

[43] BaBar Collaboration (B. Aubert *et al.*), *Phys. Rev. Lett.* **91**, 161801 (2003).

[44] M. Beneke, M. Neubert, *Nucl. Phys.* **B651**, 225 (2003).

[45] M. Gronau, D. London, *Phys. Rev. Lett.* **65**, 3381 (1990).

[46] M. Gronau, *Phys. Lett.* **B265**, 389 (1991); L. Lavoura, *Mod. Phys. Lett.* **A7**, 1553 (1992).

[47] M. Gronau *et al.*, *Phys. Rev.* **D52**, 6374 (1995).

[48] CLEO Collaboration (D. Cronin-Hennessy *et al.*), *Phys. Rev. Lett.* **85**, 515 (2000).

[49] BaBar Collaboration (B. Aubert *et al.*), *Phys. Rev. Lett.* **89**, 281802 (2002).

[50] BaBar Collaboration (B. Aubert *et al.*), *Phys. Rev. Lett.* **91**, 021801 (2003).

[51] BELLE Collaboration (K. Abe *et al.*), *Phys. Rev.* **D66**, 092002 (2002); Belle-conf-0311, LP03-ID 264, 13 pp (2003).

[52] BaBar Collaboration (B. Aubert *et al.*), SLAC-PUB-9303, `hep-ex/0308012`.

[53] Belle Collaboration (K. Abe *et al.*), BELLE-CONF-0354, 9pp (2003).

[54] BaBar Collaboration (B. Aubert et al.), SLAC-PUB-9304, `hep-ex/0207065`.

[55] P. Burchat *et al.*, Snowmass Summer Study, eConf C010630, E214 (2001).

[56] Belle Collaboration (K. Abe *et al.*), *Phys. Rev. Lett.* **89**, 071801 (2002); *Phys. Rev.* **D68**, 012001 (2003).

[57] M. Beneke *et al., Nucl. Phys.* **B606**, 245 (2001).

[58] CLEO Collaboration (A. Bornheim *et al.*), *Phys. Rev.* **D68**, 052002 (2003).

[59] M. Gronau, D. Wyler, *Phys. Lett.* **B265**, 172 (1991).

[60] BaBar Collaboration (B. Aubert *et al.*), SLAC-PUB-10220, `hep-ex/0311032`.

[61] I. Dunietz, *Phys. Lett.* **B427**, 179 (1998); I. Dunietz, R.G. Sachs, *Phys. Rev.* **D37**, 3186 (1988).

[62] BaBar Collaboration (B. Aubert *et al.*), SLAC-PUB-10155, `hep-ex/0309017`.

[63] D.G. Hitlin, invited talk at B physics day at SLAC, March 20 (2003).

[64] G.P. Dubois-Felsmann, D.G. Hitlin, F.C. Porter, G. Eigen, `hep-ph/0308262`; G. Eigen *et al.*, Proc. of Int. Europhys. conf. in Aachen, July, 2003.

[65] A. Ali, E. Lunghi, *Eur. Phys. J.* **C26**, 195 (2002).

[66] D. MacFarlane, invited talk at SLAC colloquium, May 29, 2003.